

# Damage identification of a jacket support structure for offshore wind turbines

Zhiyu Jiang  
Department of Engineering Sciences  
University of Agder  
Grimstad, Norway  
zhiyu.jiang@uia.no

Wenbin Dong  
DNV GL  
Høvik, Norway  
Wenbin.Dong@dnvgl.com

Marius Bjørnholm  
Department of Engineering Sciences  
University of Agder  
Grimstad, Norway  
mariusbjornholm@gmail.com

Zhengru Ren  
Department of Marine Technology  
Norwegian University of Science and  
Technology  
Trondheim, Norway  
zhengru.ren@ntnu.no

Jiamin Guo  
School of Ocean Science and  
Engineering  
Shanghai Maritime University  
Shanghai, China  
jmguo@shmtu.edu.cn

Amrit Shankar Verma  
Department of Aerospace Structures  
and Materials  
Delft University of Technology  
Delft, The Netherlands  
A.S.Verma@tudelft.nl

**Abstract**—Offshore jacket structures are regarded as a suitable type of support structure for offshore wind turbines in immediate water depths. Because of the welded tubular members used and environmental conditions, offshore jackets are often subjected to fatigue damages during their service life. Underwater sensors can provide measurements of the structural vibration signals and provide an efficient way to detect damages at early stages. In this work, simplified forms of the damages are assumed, random damages are imposed on the jacket structure, and damaged indicators are established from combination of modal shapes. Then, a response surface is constructed mapping the damage indicators and damages. Given that the efficiency of the damage identification depends on the locations of the damages and the location and number of sensor locations, a sensitivity study is performed to vary sensor location, sensor quantity, and damage severity. It is found that the effect of damage identification is better when sensor locations are closer to damage locations, and this effect is more sensitive to sensor placements when damages occur in the upper structures. Additionally, the identification effect is more sensitive to damage severity than to occurrence of multiple damages.

**Keywords**—*damage identification; jacket; structural modal analysis; artificial neural network; sensor.*

## I. INTRODUCTION

The offshore wind industry has been booming in the past decade. In 2018, Europe connected 409 new offshore wind turbines to the grid across 18 projects [1]. Among the various types of support structures for offshore wind turbines (OWTs), jackets were the second most used substructure, representing 24.5% of all foundations installed as of 2018 [1]. A typical offshore jacket support structure consists of slender steel structural members welded at tubular joints. Compared to other offshore structures like monopiles, jacket structures are subjected to minimal wave impacts because of the small cross section in the splash zone. Accordingly, jacket supported OWTs have the potential to be deployed at water depths beyond 50 meters. However, the development of jacket-supported offshore wind farms also faces challenges during manufacturing and onshore storage [2]. Fatigue failure of jacket structures due to welded joints is another problem. To avoid premature failures, efforts have been made to predict the fatigue life accurately and to make reliability-based inspection planning at an early stage of a project [3, 4]. For example,

Dong et al. [5] performed long-term fatigue analysis of welded multi-planar tubular joints for a jacket OWT in a water depth of 70 m, and dynamic response analysis is often involved because of the complexity of dynamic loads [6]. This document and are identified in italic type, within parentheses, following the example. Some components, such as multi-leveled equations, graphics, and tables are not prescribed, although the various table text styles are provided. The formatter will need to create these components, incorporating the applicable criteria that follow.

On the other hand, damage identification based on sensor measurements provide another effective means for early detection of damages. Given that the dynamic properties of a structure like eigenmodes and eigenfrequencies are affected by the change in structural details, such properties, if measurable, could be utilised further in damage detection using an inverse method. Asgarian et al. [7] used the rate of signal energy of wavelet packet transform as a damage index and used measured accelerations of sensors to compute the damage indices. Mangalathu et al. [8, 9] considered various machine learning techniques to identify the failure modes of beam-column joints and to estimate the shear strength. Guo et al. [10] applied artificial neural networks (ANNs) to examine the model updating of a suspended dome considering both experimental and numerical models. In another work, Guo et al. [11] proposed using partial modal results in the damage identification of offshore jackets and found that the prediction errors are sensitive to damage locations. These works demonstrate that machine learning methods together with numerical or experimental data can provide good estimate of damages.

To reduce the operation and maintenance costs of jacket supported OWTs, we can consider the use of sensors for measuring the vibration signals of support structures and apply mathematical models to detect early failures. Because reliable off-the-shelf sensors like global positioning systems (GPS) and inertial measurement units (IMU) are expensive [12], it is interesting to know if minimum number of sensors can be used and how the damage identification results vary in different damage scenarios. To this end, this paper selects a representative jacket support structure of an OWT and carries out a sensitivity study applying the finite element method, a

response surface methodology and the principle of Monte Carlo Simulations. The structure of the paper is as follows. Chapter 2 discusses the methodology; Chapter 3 presents a case study for a 5-megawatt (MW) OWT, followed by discussions of the results in Chapter 4. Finally, conclusions are drawn in Chapter 5.

## II. METHODOLOGY

### A. Damage Identification indices

The basic equation for structural modal analysis is known to be

$$(K - \omega_i^2 M)\varphi_i = 0 \quad (1)$$

where  $K$  and  $M$  are respectively the structural stiffness matrix and mass matrix. For submerged parts, the mass matrix should include hydrodynamic added mass.  $\omega_i$  and  $\varphi_i$  denote the  $i$ th-order structural eigenfrequency and modal shape, respectively. Because of the orthogonality of the modal shapes, we can express the square frequency as

$$\omega_i^2 = \varphi_i^T K \varphi_i / \varphi_i^T M \varphi_i \quad (2)$$

In the presence of structural damage, if the total stiffness matrix,  $K$  changes by  $\Delta K$  and the square frequency and modal shape change by  $\Delta\omega_i^2$  and  $\Delta\varphi_i$ , respectively, then (1) can be rewritten as

$$(K + \Delta K - (\omega_i^2 + \Delta\omega_i^2)M)(\varphi_i + \Delta\varphi_i) = 0 \quad (3)$$

Ignoring the high-order terms, (3) can be simplified as

$$\Delta\omega_i^2 = \varphi_i^T \Delta K \varphi_i / \varphi_i^T M \varphi_i \quad (4)$$

If the square frequency of the intact structures is defined as  $\omega_{ui}^2$ , then the relative difference of the square frequency for the  $i$ th-order can be expressed as:

$$RE_i = \frac{\Delta\omega_i^2}{\omega_{ui}^2} \approx \frac{\varphi_i^T \Delta K \varphi_i}{\varphi_i^T K \varphi_i} \quad (5)$$

The difference for the  $i$ th modal shape can be expressed as

$$\Delta\varphi_i = \varphi_{di} - \varphi_{ui} \quad (6)$$

where  $\varphi_{di}$  and  $\varphi_{ui}$  are the  $i$ th-order modes for the damaged structure and the intact structure, respectively. For offshore structures like jackets, underwater sensors can be installed to measure nodal displacements and modal results. Although the high-order modes are more sensitive to structural damages than the low-order modes [13], accurate high-order modal results are often difficult to obtain possibly due to measurement errors and noise. The large number of damage indices also makes it difficult for data training. Accordingly, we consider partial modal results as suggested by Guo et al. [11] in this work. The sum of the first  $n$  modal results at each measurement position is expressed as the simplified damage index as follows

$$\Delta\Psi_i = \sum_{j=1}^n \Delta\varphi x_i^j + \sum_{j=1}^n \Delta\varphi y_i^j + \sum_{j=1}^n \Delta\varphi z_i^j \quad (7)$$

where  $\Delta\varphi x_i^j$ ,  $\Delta\varphi y_i^j$ , and  $\Delta\varphi z_i^j$  are the  $j$ th-order modal shape difference for the  $i$ th measurement position in the  $x$ -,  $y$ -, and  $z$ -directions, respectively.

### B. Damage identification method

The damage identification method applied here can generally be referred to as an inverse method, because we would like to estimate the damage based on measurable damage identification indices as the input parameters.

Response surface methods [14] can be applied to establish the mapping between the input and output parameters. Common response surfaces (RS) are polynomials, Kriging models, and ANNs. Applications of RS in offshore engineering can be found in [15-17]. In this work, we considered backpropagation neural networks to represent the RS, and used the combined damage index  $[RE, \Delta\Psi]$  and the element damages ( $\Delta E$ ) as the training data for the networks. Here, the element damage is defined as the ratio of the young's modulus between the damaged and intact structural elements:

$$\Delta E_i = E_{di} / E_{ui} \quad (8)$$

Note that the ratio will lie between 0 and 1. Fig. 1 illustrates the damage identification process, where the structure of the ANNs can be identified by trial and error. When the RS is established by a set of training data, damage predictions can be made for any new input parameters.

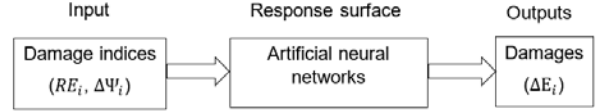


Fig. 1 Illustration of the damage identification process

### C. Procedure of analysis

Fig. 2 shows the analysis procedure considered in this work. First, a finite element model is established to perform the modal analysis of the intact structure of interest and the results are verified against literature. Second, Monte Carlo Simulations are performed, imposing random damages on specified structural members, followed by modal analysis for the intact and damaged structures. From the modal analysis, eigenfrequencies and modal shapes are obtained, and they will be further used to calculate the damage indices. The dataset will be divided into a training sample and a test

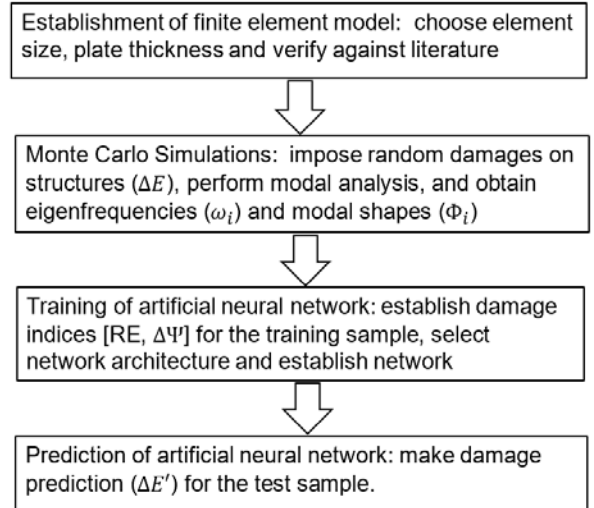


Fig. 2 Flowchart of this work

sample. The former will be used to establish the ANN structure, and the latter will be used to predict the damages.

The mean squared error (MSE) is the main metric used to calculate the summed errors between the predicted and original values of the test sample. If the sample consists of  $N$  data and is divided into  $r$  groups, and the variance of group  $i$  is  $\sigma_i^2$ , then MSE can be expressed as

$$\text{MSE} = \frac{\sum_{i=1}^r (n_i - 1) \sigma_i^2}{N - r} \quad (9)$$

### III. CASE STUDY

In this chapter, a case study of a 5-MW OWT is presented. The finite element modelling details are introduced, and the numerical study is described.

#### A. Description of the jacket-supported offshore wind turbine

As shown in Fig. 3 (left), a traditional jacket supported OWT has a rotor, a tower, a heavy transition piece, tubular members and leg piles. Fig. 3 (right) shows the support structure of a four-legged 5-MW jacket OWT that was originally designed for 70-m water depth in the North Sea [5]. The jacket foundation has a height of approximately 96 m and is partly submerged in seawater.

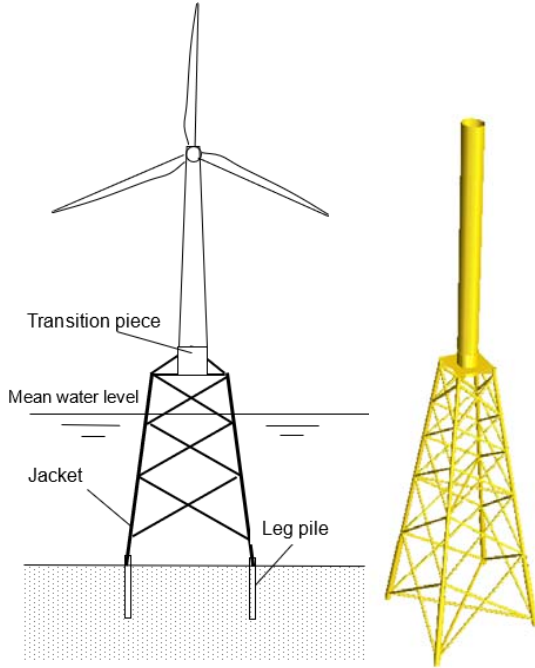


Fig. 3 Schematic of a jacket support structure for an offshore wind turbine

#### B. Finite element modelling

The support structure excluding the nacelle or the blades is modelled using the APDL programming language provided by ANSYS [18]. The PIPE59 element type with tension-compression, torsion, and bending capabilities was selected for the bracings. This element type has six degrees of freedom at each node. The welds were not modelled explicitly. A Poisson's ratio of 0.3 and a density of  $7850 \text{ kg/m}^3$  were applied for the steel members. For the intact jacket, a young's modulus of  $2.1 \times 10^{11} \text{ Pa}$  for the steel members is

considered. A convergency study is carried out to determine the mesh size, and a mesh size of 0.2 m was considered. The soil-pile interaction of the jacket piles was not modelled, and the jacket structure is assumed to be rigidly fixed to the seabed in this paper. The influence of soil-pile interaction on the structural eigenfrequencies is expected to be small [5].

#### C. Sensor location and imposed damages

Although the underwater sensors can be installed at any locations, we focus on the nodal points of the jacket structure, as these points can be more sensitive to the global modes of the structure. Fig. 4 illustrates the top, centre, and bottom locations of the sensors. For each case, 12 sensors, marked by green dots, are shown. We did not consider random sensor locations here but gradually increase or decrease the sensor numbers in the sensitivity study. It is intuitive that the more sensors, the more effective the damage identification. For installation and maintenance purposes, sensors close to the waterline are preferred.

In the numerical study, random damages were imposed on the damaged structural members by modifying the young's modulus by Monte Carlo Simulations. For most cases, the damage severity denoted by the ratio according to Equation (6) lies between 0 and 0.5. For the cases with severe damages, the damage severity is between 0.5 and 1.0, depending on the random number generated. Both specified damage locations and random damage locations were considered in the analysis.

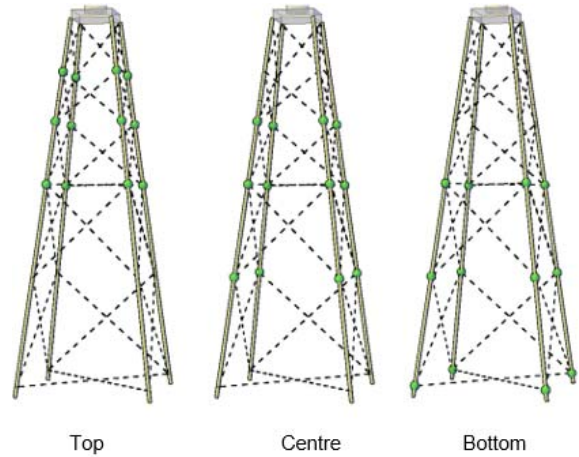


Fig. 4 Illustration of the three sensor locations considered in this work

#### D. Training and testing of samples

As aforementioned, a training sample will be used for training of the ANNs with the purpose of reducing the errors between actual damages and predicted damages. Then, the trained ANNs will be applied to predict new damages given new inputs. For each scenario, 10000 testing data and 2000 training data were selected for the training and testing samples, respectively, after a preliminary study. Further increase in the testing sample leads to better prediction effect but may also involve additional computational time. For the ANNs, the sigmoidal function was selected as the activation function, and a three-layered structure was determined. The numbers of neurons for the input, hidden, and output layer are 18, 17, 8, respectively. This structure was determined by trial and error.

## IV. RESULTS AND DISCUSSION

### A. Validation of the structural model

As structural eigenmodes and eigenfrequencies are of most interest, modal analysis of the intact jacket support structure was carried out, and the first six modal shapes are presented in Fig. 5. As shown, the first four modes correspond to global mode shapes including side-side and fore-aft modes, whereas the fifth mode has a local mode with bending of a horizontal bracing. As the jacket structure is symmetrical about the z-axis, some mode shapes have the same magnitude in the tower-top offset.

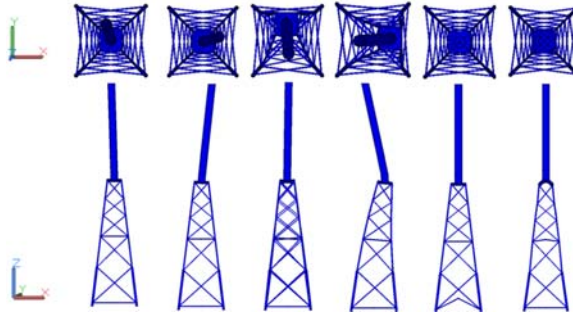


Fig. 5 Illustration of the first six modal shapes of the jacket structure

Table 1 Comparison of the eigenfrequencies of the present model and [5].

	First eigenmode (Hz)	Second eigenmode (Hz)
Present model	0.3575	1.6821
Reference	0.3486	1.6863
Relative difference (%)	2.55	0.25

Table 1 compares the first and second eigenfrequencies of the modelled support structure with the reference. The relative differences for both modes are less than 3% and can be deemed acceptable. Thus, the present structural model, mesh size, and element types are further used in damage identification.

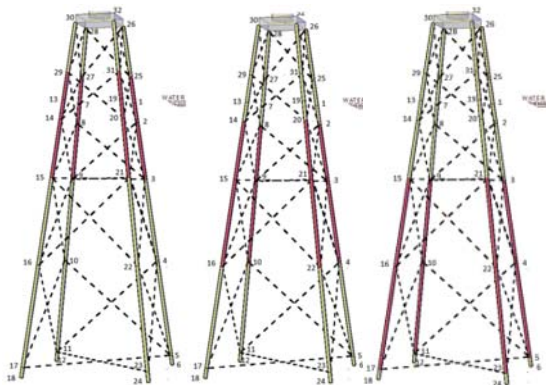


Fig. 6 Illustration of eight damaged members at the top, in the middle and at the bottom (from left to right)

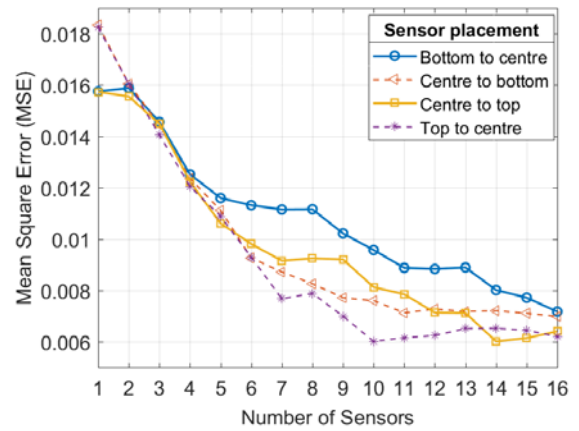


Fig.7 Variation of mean square error with sensor number, with eight damaged members at the top

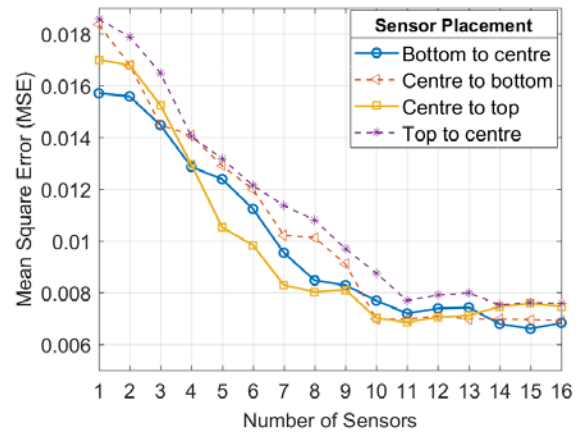


Fig. 8 Variation of mean square error with sensor number, with eight damaged members in the centre

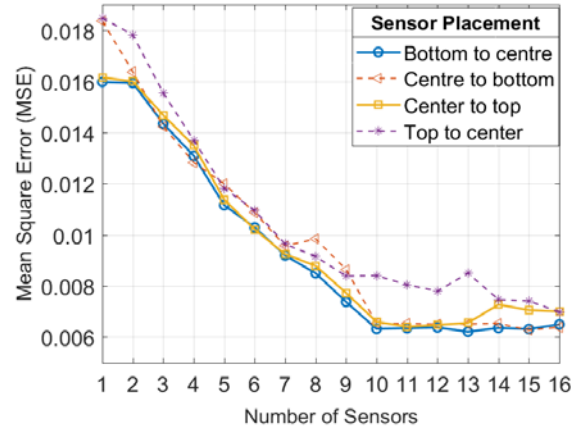


Fig. 9 Variation of mean square error with sensor number, with eight damaged members at the bottom

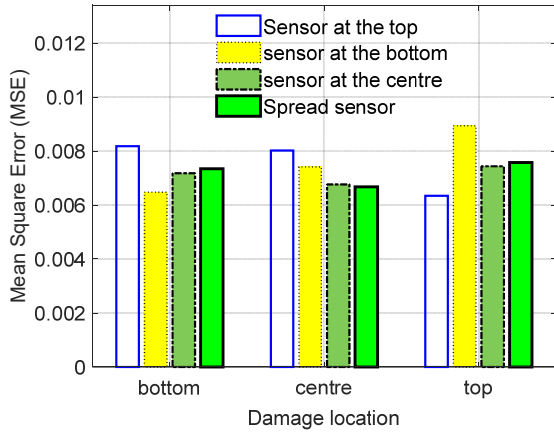


Fig. 10 Effect of sensor location on the mean square error of damage

**B. Effect of sensor location and sensor number on damage identification**

Specified damaged members at different locations of the jacket are illustrated in Fig. 6. For these members, the variation of MSE with sensor location and sensor number is shown. The sensor number is increased from 1 to 16. In the legends of Figs. 7-9, “top to centre”, “centre to bottom”, “centre to top”, and “bottom to centre” refer to the order of sensor number increment. The sensors are initially placed at the top nodal points. For example, for “top to centre” in Fig.7, the first four sensors are placed at nodes 31, 25, 27, 29, respectively, followed by nodes 19, 1, 7, 13 if the sensor number rises to eight. For the case of eight damaged members at the top (Fig.7), the MSE for the sensor placement of “top to centre” stays the lowest among the four placements. This is reasonable as the damage identification effect is expected to be good when the damages occur in proximity to the sensors. Comparing the three figures for a sensor number, the effect of the sensor placements on MSE appears to be the smallest when the damaged members are in the bottom. This observation is probably because damages in the upper structural parts result in greater changes in the modal information, as indicated by the modal shapes and boundary conditions. Since this study assumes random occurrence of damages, the top sensor placement is preferred. Another question arises about the proper sensor number. In general, the MSE experiences a steep descent when the sensor number increases from 1 to 10. Further increase in the sensor number may still slightly improve the MSE with additional costs.

Fig. 10 presents the MSE results considering 12 sensors with varying sensor and damage locations. The observation is in line with previous figures, as MSE continues to be lowest when sensor and damage locations are close. The spread sensor scenario is included in addition. As shown, when the 12 sensors are spread over the jacket structure, the average MSE maintains the minimum. Although this can be difficult in practice, the industry should evaluate this option when considering damage identification.

**C. Sensivity to damage severity**

Here, 12 sensors are assumed to be installed either at the top or at the centre, but damages are imposed on random structural members; see Fig. 11 for the case of three and four damaged members. Two levels of damage severity are considered. The first level has light damages with 0-50%

changes in the steel’s young’s modulus and the second level has severe damages with 50-80% changes in the young’s modulus. As shown in Fig. 12, MSE has a substantial decrease when the severity level increases, indicating the potential improvements in the damage prediction accuracy. As the damaged members are randomly selected, there is limited difference between the two predetermined sensor locations. Interestingly, for both damage levels, the MSE does not change too much when the number of damaged members increase from 1 to 4. This indicates that the damage identification approach is valid for different damage scenarios.

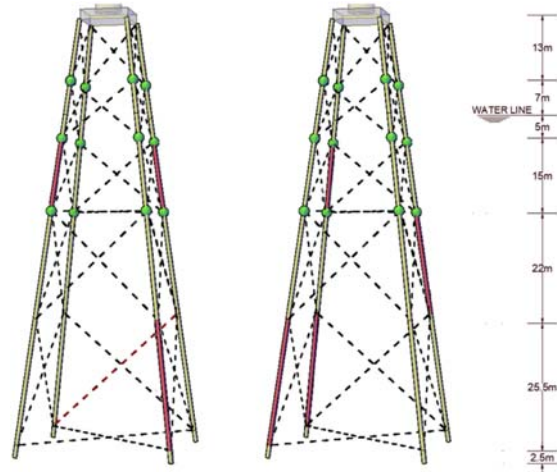


Fig. 11 Schematic of 12 sensors located at the top and random damage locations (left: three damaged members; right: four damaged members)

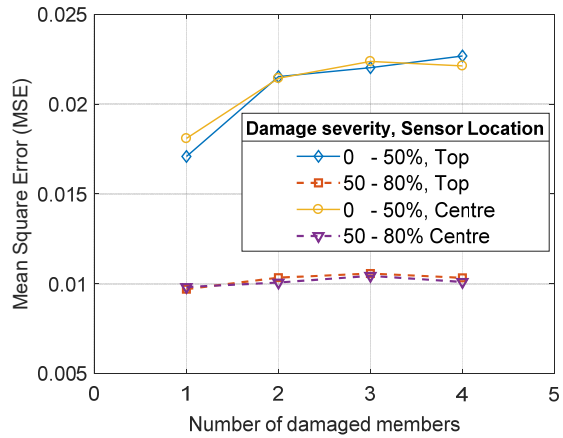


Fig. 12 Effect of damage severity on damage identification with varying number of damaged elements

## V. CONCLUSION

This paper presents a damage identification of a jacket support structure of an offshore wind turbine. Artificial neural networks are used to establish the response surface which correlates the damage indices with damages. A sensitivity study is carried out in a finite element program, assuming simplified forms of damages and imposing random damages on the structural members. Based on the study, the following conclusions are drawn:

- When damages are in the upper regions of the jacket structure, the influence of sensor placement on the sensitivity of the mean square error of damage identification is relatively small.
- The damage identification method achieves good results when the damages occur in the proximity to sensor placements.
- The damage identification effect is affected by the number of sensors used, especially when the sensor number is small. More than 10 sensors should be used for damage identification purposes. Note that for a jacket of different sizes, this number may also change.
- For a given number of randomly selected damaged members, the effect of damage identification is improved significantly when the damage severity increases.

## VI. FUTURE WORK

This work presents an application of a damage identification approach to the jacket-supported offshore wind turbines. The wind turbine components including blades and nacelle are not included in the structural model. It is interesting to further verify this approach in damage identification of blade or drivetrain components. As the jacket structure is primarily submerged underwater, the hydrodynamic added mass is expected to affect the modal modes and frequencies [19]. This work does not examine the influence of added mass on the damage identification, either. This aspect is relevant for practical deployment of jacket wind turbines. Finally, simplified assumptions are made for the damages by reducing the young's modulus and by considering random damages throughout the structure. These simplifications can be improved by more realistic considerations in future.

## ACKNOWLEDGMENT

The contributions of Martin Salvesen, Marius Nielsen, and John Morgan Larsen of University of Agder are acknowledged for their bachelor thesis work.

## REFERENCES

- [1] C.E. Walsh, Offshore wind in Europe key trends and statistics 2018. 2018, Wind Europe.
- [2] K. Thomsen, *Offshore wind: a comprehensive guide to successful offshore wind farm installation*. 2014: Academic Press.
- [3] Z. Jiang, W. Hu, Z. Gao, W. Dong, and Z. Ren, *Structural reliability analysis of wind turbines: a review*. Energies, 2017. **10**(12): p. 2099.
- [4] T. Lassen and N. Recho, *Fatigue life analyses of welded structures*. 2006., ISTE Ltd, UK.
- [5] W. Dong, T. Moan, and Z. Gao, *Long-term fatigue analysis of multi-planar tubular joints for jacket-type offshore wind turbine in time domain*. **33**(6), 2002-2014.
- [6] Z. Jiang, Y. Xing, Y. Guo, T. Moan, and Z. Gao, *Long-term contact fatigue analysis of a planetary bearing in a land-based wind turbine drivetrain*. Wind Energy, 2014. **18**(4), 591-611.
- [7] B. Asgarian, V. Aghaeidoost, and H.R. Shokrgozar, *Damage detection of jacket type offshore platforms using rate of signal energy using wavelet packet transform*. Marine Structures, 2016. **45**: p. 1-21.
- [8] S. Mangalathu, G. Heo, and J.S. Jeon, *Artificial neural network based multi-dimensional fragility development of skewed concrete bridge classes*. Engineering Structures, 2018. **162**: p. 166-176.
- [9] S. Mangalathu and J.S. Jeon, *Classification of failure mode and prediction of shear strength for reinforced concrete beam-column joints using machine learning techniques*. Engineering Structures, 2018. **160**: p. 85-94.
- [10] J. Guo, X. Zhao, J. Guo, X. Yuan, S. Dong., and Z. Xiong, *Model updating of suspended-dome using artificial neural networks*. Advances in Structural Engineering, 2017. **20**(11): p. 1727-1743.
- [11] J. Guo, J. Wu, J. Guo, and Z. Jiang, *A damage identification approach for offshore jacket platforms using partial modal results and artificial neural networks*. Applied Sciences, 2018. **8**(11): p. 2173.
- [12] Z. Ren, R. Skjetne, Z. Jiang, Z. Gao, and A.S. Verma, *Integrated GNSS/IMU hub motion estimator for offshore wind turbine blade installation*. Mechanical Systems and Signal Processing, 2019. **123**: p. 222-243.
- [13] M. Radziński, M. Krawczuk, and M. Palacz, *Improvement of damage detection methods based on experimental modal parameters*. Mechanical Systems and Signal Processing, 2011. **25**(6): p. 2169-2190.
- [14] R.H. Myers, D.C. Montgomery, and C.M. Anderson-Cook, *Response surface methodology: process and product optimization using designed experiments*, 3rd ed. Vol. 705. 2009, Hoboken, New Jersey, USA: John Wiley & Sons,
- [15] Z. Jiang, *The impact of a passive tuned mass damper on offshore single-blade installation*. Journal of Wind Engineering and Industrial Aerodynamics, 2018. **176**: p. 65-77.
- [16] L. Li, Z. Jiang, M.C. Ong, and W. Hu. *Design optimization of mooring system: an application to a vessel-shaped offshore fish farm*. Engineering Structures, 2019. **197**: p. 109363.
- [17] A.S. Verma, Z. Jiang, Z. Ren., Z. Gao, and N.P. Vedvik, *Response-based assessment of operational limits for mating blades on monopile-type offshore wind turbines*. Energies, 2019. **12**(10), p.1867.
- [18] P. Kohnke, *ANSYS theory reference manual*. Ansys Inc., Canonsburg, PA, USA, 2013.
- [19] H. Moll, F. Vorpahl, and H.-G. Busmann. Dynamics of support structures for offshore wind turbines in fully-coupled simulations-influence of water added mass on jacket mode shapes, natural frequencies and loads. in European Wind Energy Conference (EWEC). Fraunhofer Institute for Wind Energy and Energy Systems Technology IWES. 2010.